Review

Jet Feedback in Star-Forming Galaxies

Martin G. H. Krause

Centre for Astrophysics Research, Department of Physics, Astronomy and Mathematics, University of Hertfordshire, College Lane, Hatfield AL10 9AB, UK; m.g.h.krause@herts.ac.uk

Abstract: In this paper, I review our understanding of how jet feedback works in star-forming galaxies. There are some interesting differences to radiative feedback from Active Galactic Nuclei (AGN). Jets act on galaxy haloes as well as on dense gas, for example in regularly rotating discs, where they can suppress star formation (particularly in the centre, negative feedback), but also enhance it (positive feedback). Jet feedback may produce turbulent, multi-phase gas structures where shocks contribute to the ionisation and is observed in connection with galactic outflows. The exact driving mechanism of these outflows is still unclear, but may be a combination of effects linked to star formation, jet-induced turbulence and radiative AGN feedback. Supermassive black holes in any galaxy can produce jets. Preferential radio detections in more massive galaxies can be explained with different conditions in the circumgalactic medium and, correspondingly, different jet–environment interactions.

Keywords: galaxy evolution; active galactic nuclei; jets

1. Introduction

Understanding the effect of feedback via Active Galactic Nuclei (AGN) on the evolution of galaxies is a major challenge in astrophysics. Arguments for an important role of the central supermassive black hole (SMBH) include the correlation between the SMBH mass M and the mass and velocity dispersion σ of the spheroidal component of the host galaxy [1–9], which can be interpreted as the outbursts of black holes of a certain size only being able to quench star formation in a given galaxy [10,11]. Recent simulations explore this in much detail, also finding ways of co-evolution of black holes and galaxies that do not involve AGN feedback [12], but typically do require AGN feedback, at least for massive galaxies $\gtrsim 10^{10} M_\odot$, e.g., [13–15]. Another argument is the need for additional feedback beyond the one from star formation to limit galaxy growth to observed masses in cosmological models [16–22]. AGN, including radio AGN, while rare among the entire population of galaxies, are found frequently enough with sufficient power to make the scenario of AGN feedback energetically plausible [23–27]. This evidence includes radio AGN in dwarf galaxies [28]. Evidence for the effect of radio jets on hot gas around galaxies has been seen directly with X-ray imaging [29–31] and is implied from the formation of fat radio lobes e.g., [32,33].

AGN feedback via jets, sometimes called radio mode feedback, has some important physical differences compared to the quasar mode, which is linked to the radiative output of the AGN. In the quasar mode, relatively dense gas around the AGN is accelerated via radiation pressure e.g., [34–39], subject to instabilities [40–45], gravity and interaction with the environment e.g., [46,47]. The radiation force acts mainly in the ionisation cones and declines away from the SMBH as r^{-2}. It is hence strongest in the centre of the galaxy. Jets can interact directly with dense gas in a galaxy to a varying degree, depending on their inclination. After breakout from any dense interstellar medium (ISM) they can then channel the feedback energy far away from the AGN, so that it can interact for example with circumgalactic gas, or, if the galaxy is a member of a cluster, the intracluster medium, with indirect effects on the host, and potentially other galaxies [48]. The physics of jet feedback is thus different from the one of radiative AGN.

This review is structured from small to large scales. After a general introduction to jet physics and the physics of the jet–environment interaction (Section 2), I first review jet feedback in the central kpc of a galaxy (Section 3), and then discuss the scale of an entire galaxy including jet-induced star formation (Section 4). Section 5 covers emission line lobes and the alignment effect, which have been connected to outflows and jet-induced star formation outside the host galaxies. Another feature of high-redshift radio galaxies are associated absorption line systems, which have been interpreted as halo shock waves from starburst winds preceding the jet event (Section 6). The contribution of jets to the heating of galactic gas halos and thus prevention of gas cooling and condensation in the host galaxy is discussed in Section 7.

2. Jet–Environment Interaction in General

A jet channels energy away from an AGN and transfers it to gas phases of interest when and where it interacts with them. Evidence for this jet–environment interaction is seen directly in the hotspots of extragalactic radio sources e.g., [49–51]. There is good evidence that AGN jets are generally relativistic on parsec scales [52–57], hence supersonic with respect to their ambient medium. Jets are likely initially accelerated as well as collimated by magnetic fields e.g., [58,59]. Hydrodynamic interaction with the ambient medium takes over the collimation at some radius, possibly even on the parsec scale [60,61]. The ambient gas pressure then drives a recollimation shock into the beam, which leads to a stable, cylindrical jet, if the opening angle from the magnetic collimation phase was not too large [62,63]. Unless there is significant entrainment, which would result in the jet slowing down, becoming unstable and disrupt [64,65], the jet velocity will remain essentially constant up to the hotspot. Hotspots are therefore best interpreted as shocks where the high bulk velocities are isotropised and electrons are accelerated to high Lorentz factors, such that they become observable via synchrotron radiation e.g., [66,67]. Hotspots are high-pressure regions that will expand and inflate the radio lobes, whenever the jet density is significantly below the ambient density [68,69]. All three components, jets, hotspots and lobes, are clearly visible on radio images of a large number of extragalactic radio sources, for a review see [31]. Radio lobes are initially strongly overpressured and drive a fairly spherical shock wave into the ambient medium around the radio source [33,70]. The shock's structure then elongates as the sideways Mach number drops [71]. Many observed radio galaxies are close to pressure equilibrium sideways and have very weak shocks around them, except near the hotspots [72,73]. An overview sketch can be found in Figure 1. Jets interact with different components of the host galaxy ISM in different ways, which I address in turn in the following.
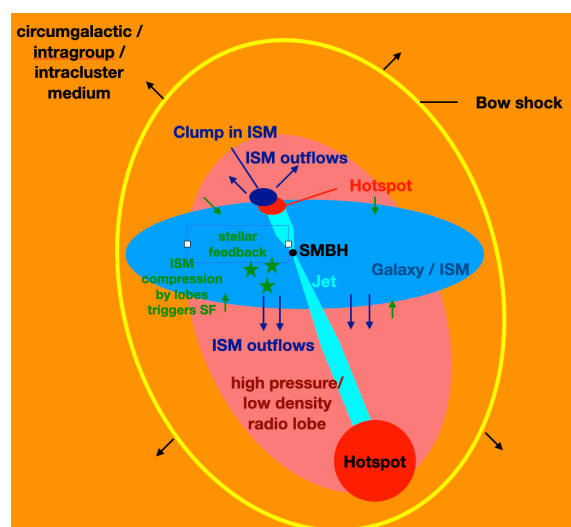

Figure 1. Schematic of features expected in connection with radio-mode feedback in star-forming galaxies. Jets are produced from supermassive black holes (SMBH). The ISM in star-forming galaxies

contains dense clumps and molecular clouds. Jet interaction with clouds is stochastic, hence the two jets emerge at different times from the ISM with, in general, a length asymmetry. The interaction in the centre may launch an outflow of the central ISM. Hotspots form at the current jet–environment working surfaces. These high-pressure regions expand, forming the radio lobes which can still be overpressured with respect to the environment. Radio lobes can compress the host galaxy's ISM, thus enhancing star formation. Stellar feedback may also launch outflows of dense gas into the radio lobes, which can then turbulently entrain them and move them by buoyancy to larger distances from the galaxy, especially when the radio source turns off. As long as the radio lobes are overpressured, they drive a bow shock into the surrounding gas which helps keep the latter hot. Turbulence in the lobes drives weak shocks into the gas around the lobes, which might also dissipate heat into this gas.

3. The Central Kiloparsec

The ISM in the central parts of galaxies can be complex, for example shaped by bars, if present e.g., [74]. The gas dynamics can lead to suppressed star formation in regions of low gas density or shear, or strong star formation in regions of gas accumulation. In the Milky Way, an example for a barred galaxy, the gas density is approximately constant with radius down to the bar end at a few kpc, then dips by a factor of approximately two and then peaks up strongly in the central kpc, the so-called central molecular zone [75]. This region probably undergoes a cyclic behaviour with periods of re-filling with gas channeled down by the bar, and repeated starbursts [76].

The central kpc is of particular significance for the jet–environment interaction in galaxies, because the size is comparable to the scale height of the neutral ISM, typically a few hundred parsecs [77–80]. Jets are expected to interact strongly with the clumpy ISM in galaxies while contained in it. This is well-studied in nearby jetted Seyfert galaxies. MRK 78 is an excellent example [81], where the knotty structure in radio continuum as well as optical emission lines suggest strong and localised interaction between the jets and the clumpy ISM. Other examples include NGC 4151 [82,83] and NGC 5929 [84,85]. Sources of these sizes in general are well-known from radio observations as peaked spectrum sources and compact symmetric objects, with common spectral features that can be well-explained by absorption from a dense ISM [86,87].

Jets interacting with the clumpy media likely present in the centres of many star-forming galaxies have been modelled in hydrodynamic simulations e.g., [88–94]. The strong interaction with clumps is also seen in such simulations. In general, the relativistic jet plasma is efficiently isotropised by jet–cloud interactions. The shocked high-pressure plasma drives a shock wave through the ISM. The result is a complex combination of cloud acceleration, ablation and compression, both triggering and suppressing star formation. If the jet is directed into the disc of a star-forming galaxy, the interaction will lead to a general expansion of the ISM with strong kinematic perturbations of the gas, and this is in good agreement with observations of line kinematics in at least the well-studied case of IC 5063 [95]. The energy transfer from the jet to cloud kinetic energy is of the order of 20–30 per cent in this phase [89,94]. The momentum transfer for any given direction exceeds unity, because the pressure of the shock-heated jet and ambient plasma produces additional momentum compare also [96], the mechanical advantage. The different directions cancel, of course, if one takes the sum, to conserve momentum overall. This phase takes about 10^5–10^6 yrs for jets with typical energy fluxes (10^{43-46} erg/s), possibly longer, if the jet is oriented in the disc plane [94,95]. After the jet has broken out of the dense ISM of a galaxy, the centre is predicted to have a significantly reduced gas density e.g., [97], perhaps with the exception of very central and dense components. A shock is driven from the centre into the outer parts of the ISM that may enhance star formation, and some gas is set up with enhanced kinematics to form an outflow, possibly observable in optical emission lines. The latter has nicely been demonstrated in 3D simulations by Meenakshi et al. (2022) [94]. Because the interaction with the clumpy interstellar medium is stochastic, the jets will in general have acquired a substantial asymmetry, with one jet likely being significantly longer than the counterjet [98].

On much smaller scales of the order of the scale height of the dense molecular gas ≈ 50 pc, e.g., [99], radio lobes could drive star-forming shock waves that may even produce high-velocity stars [100].

This general picture is consistent with the rapid decline of star formation inferred in the centre of some post-starburst galaxies e.g., [101,102]. The general quenching of galaxies may, however, not be strongly influenced by jet feedback, at least at low redshift, because radio AGNs appear typically only about 1.5 Gyr after the peak of a star formation episode [103,104].

4. Small Radio Galaxies and Jet-Induced Star Formation

This section is about radio galaxies with radio sizes comparable to the diameters of gaseous galactic discs (tens of kpc). Once the jets have left the dense ISM of the host galaxies they are expected to form some kind of radio lobe. How prominent they are and how well they are observable differs with generally more prominent lobes in more massive galaxies [105]. Synchrotron emission increases with both magnetic and relativistic electron pressure. Denser environments will generally provide more resistance and thus lead to higher pressure, and hence more radio emission. While the intracluster medium in galaxy clusters can reach $>10^{-2}$ cm^{-3}, the circumgalactic gas around the Milky Way, with a stellar mass $M_* \approx 6 \times 10^{10} M_\odot$ [106,107], is already at $n \approx 10^{-4}$ cm^{-3} [108]. For smaller galaxies, the virial temperature of the halo, which is the expected temperature scale for the gas, drops below 10^6 K. The volumetric cooling rate is proportional to Λn^2, with the cooling function Λ being a function of the temperature and, in general, also metallicity. Hence, any hydrostatic halo would have to be much more tenuous to prevent pressure loss from cooling for details [105]. Such halos are easily pushed to inflow or outflow states.

Radio lobes in the circumgalactic medium are nevertheless known. A likely example is the ≈ 8 kpc sized pairs of the Fermi bubbles in the Milky Way e.g., [109–112], though the radio emission was actually not observed in this case, probably due to our special location. The nearby Circinus galaxy seems to be a similar case [113], with lobe sizes of the order of one kpc. Similar detections in X-rays and gamma rays include M31 [114], NGC 891 [115], and NGC 3079 [116]. More radio detections can be expected with the SKA [117]. The luminous infrared galaxy IC 2497 (Hanny's Voorwerp) at redshift of $z = 0.05$ is one of a few spiral galaxies, with likely jet-related radio emission in the circumstellar gas tens of kpc from the nucleus, [118], where the radio emission is only seen on the side of the galaxy that seems to contain the denser gas structures. Nesvadba et al. (2021) [119] presented an analysis of the nearby massive spiral galaxy J2345-0449, which is also associated with radio lobes of 1.6 Mpc diameter. The galaxy features a massive molecular gas ring that is obviously kinematically impacted by the jet at two opposite interaction points.

Nesvadba et al. (2021) [119] reported an unusually low star formation rate and suggested the jet impact to stir the molecular gas ring and thus prevent star formation. The width of the observed ring of 24 kpc makes this appear difficult with the so far discussed mechanisms, but the authors also explain the difficulties with other, non-jet related mechanisms that might suppress star formation in this molecular ring. Many galaxy-sized radio sources are known, for example, from the 3CRR and LOFAR surveys [26], and also at high redshift $z \gtrsim 2$, e.g., [120].

When the radio source expands into the galactic halo, a radio lobe may form, if the circumgalactic gas is denser than the jet e.g., [63,68,70]. The point of highest pressure in the radio lobe is the hotspot at its tip. Therefore, there is generally a backflow in the radio lobes towards the galaxy. Gaibler et al. (2012) [121] found, in 3D hydrodynamical simulations of powerful jets developing lobes in the ISM, that the pressure of the lobes compressed the clumpy ISM in the simulated galaxy (compare Figure 2). They concluded that this likely led to star formation enhanced by a factor of a few propagating outwards from the galactic centre, as the radio lobes grow. Follow-up studies found that this phase of enhanced star formation may last for much longer than the active time of the radio source, and thus lead to more rapid gas exhaustion [122].
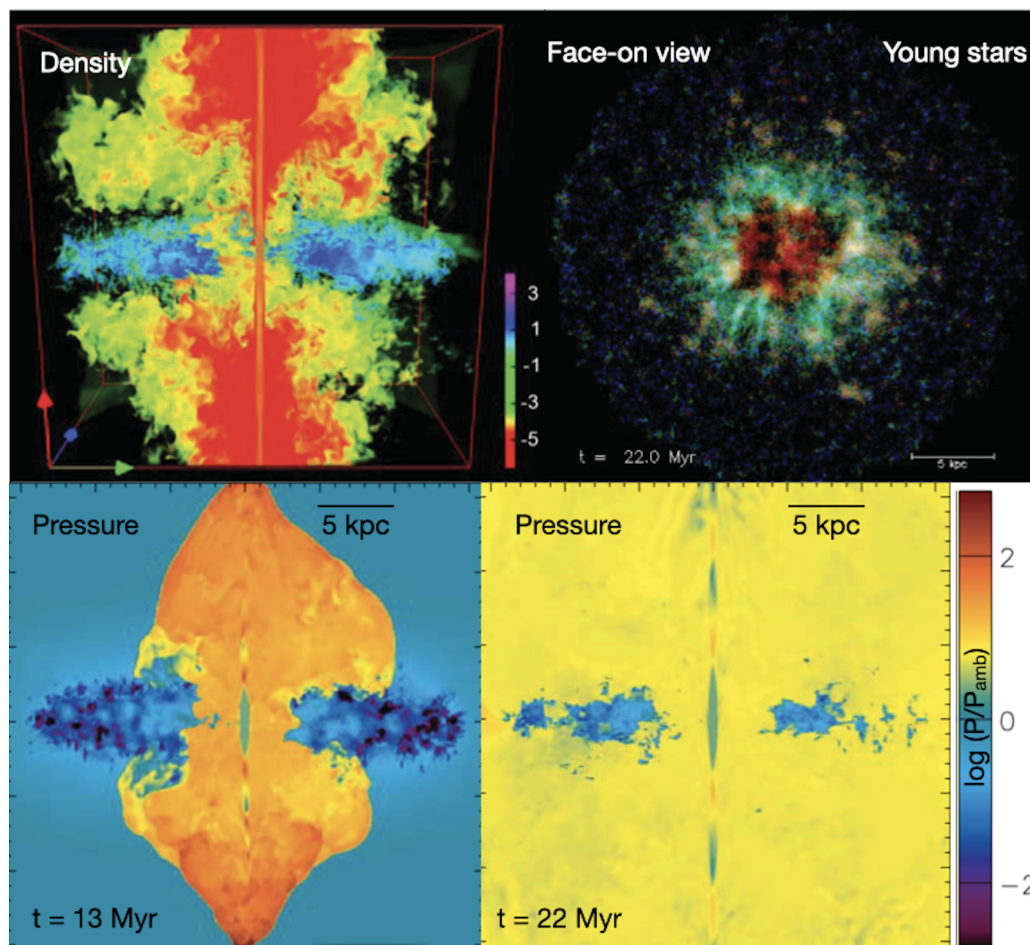
Figure 2. Hydrodynamic simulation of jet–induced star formation in a gas–rich galaxy, adopted from [121]. All panels show the evolution 12 Myr after the onset of the jet (22 Myr after start of the simulation), except the bottom left panel, which is 1 Myr after jet onset. (**Top left**): Logarithmic density volume rendering. Blue colours show the dense ISM in the modelled galaxy from the centre of which bipolar, very light jets emerge vertically upwards and downwards. Gas cooling is prevented below 10^4 K, which sets the approximate disk temperature. The radio lobes (red and yellow) surround and compress the disc. (**Top right**): Map of stars formed during the simulation. Red: stars that formed before the jet was active; green, stars formed since the jet was active, except the ones shown in blue, which are stars formed within the last Myr. The centre of the galaxy is cleared of gas, and a ring of enhanced star formation is driven outwards. Overall, the enhancement of the star formation rate peaked at a factor of a few during the simulation. About 10 percent of the gas mass was estimated to be converted to stars during one duty cycle. (**Bottom**): Pressure maps (midplane slices) 1 Myr (**left**) and 12 Myr (**right**) after jet onset. Shown is the logarithm of the ratio of the local pressure over the initial ambient pressure. In both bottom panels, the jet points upwards and downwards. Initially, jets and lobes are several orders of magnitude above the disc pressure. The overpressure is still appreciable after 12 Myr. Values in real systems will vary with jet power and halo properties.

Isolated gas clouds in the circumgalactic gas that are overrun by the jet's bow shock will experience compression, and plausibly form stars [123]. If they are also overrun by the radio lobes, they will also experience shear, be torn apart, and mix with the lobe material, thus suppressing star formation [124,125]. Regions of well-developed turbulence in the radio lobes can also enhance drop-out of cold gas, and thus, star formation [126]. As shown in 3D high-resolution zoom simulations by Krause (2008) [127], it depends sensitively on the initial conditions, such as on the initial mass loading of the radio lobes, if the cold gas mass increases or decreases. This source also derives a power estimate for emission lines that cold gas emits in a multiphase turbulence situation, such as in a radio lobe due

to shock heating and mixing. The simulations gave a cooling power of dense gas as a proxy for emission line luminosity of roughly 1 erg/s for every 10^{12} erg of turbulent kinetic energy. Meenakshi et al. (2022) [94] used a more sophisticated emission model to predict the emission for, specifically, the O III luminosity in a region of clumpy ISM impacted by a jet, and found 10^{43} erg/s peak flux for simulations with about 100 times more powerful jets. With a simulation time of ≈ 1 Myr and conversion of about 10 percent of their energy flux into kinetic energy of dense gas, this translates to a peak efficiency of 1 erg/s in O III luminosity for 10^{14} erg of kinetic energy in dense gas. Since much of the emission may be from other lines, particularly hydrogen, the order of magnitude comparison seems to be in reasonable agreement. Multiphase turbulence in radio lobes can thus sustain a certain level of dense emission line clouds, possibly leading to the alignment effect, which is discussed in the next section.

5. Emission Line Lobes and Alignment Effect

The combination of optical and radio observations that constitute the alignment effect has been reviewed, for example, in the Refs. [126,128,129]. Good examples are found in the Refs. [130–132]. Optical, nebular emission, is aligned with, and in many well-resolved cases "inside", that is close to the host galaxy on the same axis or co-spatial with the radio lobes (compare Figure 3). The observational characteristics of these sources are well-explored. Smaller radio sources ($\lesssim 100$ kpc) have more prominent emission line lobes with large bulk outflow speeds, comparable to the escape velocity of the host galaxy, and velocity widths often in excess of 1000 km/s [133]. Their emission line ratios are more consistent with shock ionisation rather than photo-ionisation by a hidden quasar (as is the case for the larger sources). The picture is consistent with a turbulent outflow, where the emission line gas might be stirred up by strong interaction of the jets with the ISM in the very early phases [97] and interaction of the turbulent backflow in the radio lobes in young ($\lesssim 100$ kpc) sources [96]. Turbulence would then have decayed in the larger scale sources, which would also lower the emission line power due to shock ionisation (compare above), such that photoionisation dominates. Another important effect is the detachment of the radio lobes due to buoyancy. In small sources, the lobes likely extend back to the host galaxy and join there, which, due to synchrotrons ageing backwards from the hotspots, can only be observed at low frequencies [134]. This can also, for example, be seen from the low-frequency radio images and associated X-ray cavities in the nearby radio galaxy Cygnus A [135,136], where the gas content and star formation rate of about 10 $M_\odot$/yr [137] is probably too low, given the high mass of the eliptical galaxy, to produce prominent emission line lobes. At around 100 kpc, powerful radio sources are expected to come into a pressure equilibrium and the lobes detach from the host galaxy, moving outwards along the radio axis [72]. The entrained gas is expected to be carried along with the radio lobes, especially later, when the source is switched off and the lobes keep buoyantly rising away from the host galaxy [138]. The surrounding hot atmosphere then flows back in where the radio lobes have left. Such dense gas is a major obstacle for galactic scale gas outflows [139–141]. It is hence very possible that emission line lobes constitute one distinct episode of a gaseous outflow in a massive galaxy: whatever mechanism ejects the dense ISM does so when the low-density radio lobes surround the galaxy. Then the radio lobes take this gas with them, when they rise away from the galaxy. This can be a major gas ejection mechanism, with derived outflowing gas masses of up to the order of $10^{10} M_\odot$ [130].

In this picture, it is probably not surprising that stars may form in such emission line lobes, when the turbulence in the lobes settles down, for example, when the lobes grow and elongate in later phases, or when the driving power of the jet declines, perhaps temporarily, for some reason. A young stellar population has been observed unambiguously with spectral features including typical absorption lines in the redshift $z = 3.8$ radio galaxy 4C41.17 [142,143].

Generally similar physics seems to be at play for lower power jet events [144], and the emission line region in the X-ray cavities of the nearby radio galaxy 3CR 196.1 could also be a similar phenomenon [145].
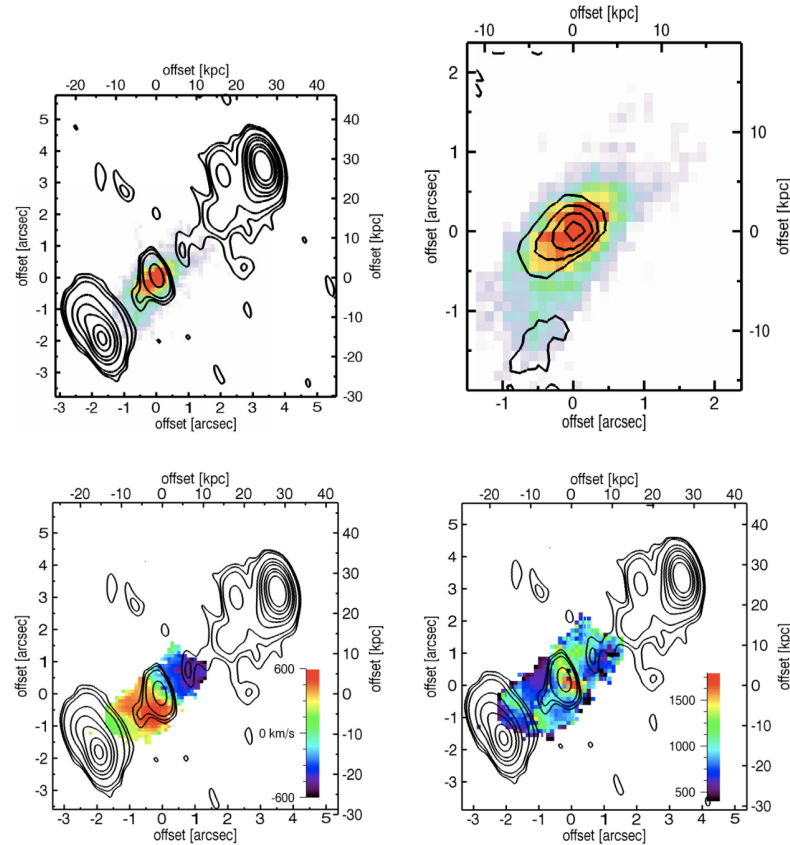

Figure 3. The radio galaxy (1.4 GHz continuum contours, except top right) MRC0406–244 at redshift $z = 2.42$ as an example for the alignment effect between radio emission and optical emission. Colours show the O III line emission (total emission: top left and right, bulk velocities: bottom left, line widths: bottom right). Contours in the top right panel show the optical continuum, which is also extended in the direction of the radio lobes. Credit: Nesvadba et al., A&A, 491, 407, 2008, reproduced with permission ©ESO [130].

6. Associated Absorption Line Systems

At the higher redshifts ($z \gtrsim 2$), emission line halos become well-observable in Ly α. A typical feature of small ($\lesssim 50$ kpc) radio galaxies is that one or more narrower absorption lines are seen against the Ly α emission [120,146]. The absorption occurs much more frequently than expected from the Ly α forest. Some absorbers were confirmed at high spectral resolution [147], and integral field spectroscopy demonstrated a coherent absorption system across the Ly α-emitting regions of several galaxies [148–150].

Different ideas for the physical interpretation of these absorption systems have been reviewed by Krause (2005) [151]. Their small velocity width suggests that they are probably thin shells around the host galaxies, rather than extended parts of the halo. The absorbers are probably partially photoionised [152,153] and their low emission suggests that the power of the process driving them into the halo is probably equally low. This makes models that use the jet as a driver of the shell [154] more difficult. A consistent scenario was developed and supported by hydrodynamic simulations in Ref. [151]. In the halos around massive high-redshift galaxies, one expects tenuous gas with a lower temperature and cooling time than in the intracluster or intragroup medium at a lower redshift, where many sources that have been observed in some detail are found. Bow shocks driven by any star-formation-related galactic wind will hence efficiently cool and sweep up the halo gas

similar to the well-known snow-plough phase for stellar winds. When a jet then hits this galactic wind shell, it is stopped for some time until the radio lobes fill the space inside the wind shell. The enhanced pressure then accelerates the wind shell, which subsequently fragments via the Rayleigh–Taylor instability. The shell gas mixes turbulently into the radio lobes while falling into the galaxy. Radio sources that are greater than the wind shells will thus experience no more associated absorption. The model is further corroborated by the discovery of similar absorption systems around high-redshift galaxies with no jets [155–158]. Such shells could also form a significant amount of stars, probably in massive clusters [154].

7. Indirect Feedback via Halo Heating

A hydrostatic, though probably tenuous gas halo may be expected in galaxies with stellar masses above $\approx 10^9 M_\odot$ [105,159]. Once the jet escapes the dense interstellar medium of the host galaxy, it may heat the halo gas and thus prevent it from cooling and subsequent condensation in the given galaxy where it could then have formed stars. Strong, close to isotropic shocks will heat a small, inner part of the halo gas, before the shock strength declines e.g., [70,72]. Changing jet direction, perhaps due to mergers of supermassive black holes after galaxy mergers, may plausibly help heating halos of gas-poor (elliptical) galaxies or the intracluster medium [160–162]. In a star-forming and therefore gas-rich galaxy, much of the jet duty cycle compare, e.g., [26,163] might be spent interacting with the ISM, rather than with the halo, if the jet axis is substantially misaligned with the minor axis of the galaxy. However, once a jet escapes the dense interstellar medium of the host galaxy, it may contribute to heating gaseous halos around star-forming galaxies in a similar way as known from the intracluster medium, including via rising bubbles and sound waves triggered by the dynamics inside radio lobes e.g., [164–166]. Taking into account the impact of jets on the surrounding gas, Rouf et al. (2017) [167] are able to explain the mass and radio luminosity functions of massive galaxies in a semi-analytical cosmological model.

Extended gas halos have been detected in Lyα around high-redshift radio galaxies beyond the radio structures [168,169]. The gas halos show quiescent kinematics with a rotating component. They have been interpreted in terms of clumps of cold gas possibly ionised by a hidden quasar in such radio galaxies. Lyman α emission is, however, also expected from hydrostatic halo gas at somewhat lower temperatures than the X-ray clusters known from lower redshifts. High-redshift radio galaxies are massive galaxies that often go through episodes of strong star formation [170,171]. It is at least plausible that cooling of halo gas strongly contributes to fuelling their star formation. The extended radio sources seen in these galaxies are evidence that halo heating is taking place in these galaxies, likely cutting off their gas supplies to at least some degree.

8. Summary

The interaction of jets with the ISM in their host galaxies is rich in interesting processes. Informed by a host of new, excellent observations and significant simulation efforts, the last few decades have seen a consistent gain in our understanding of jet feedback. We now start to be in a position where we can put together the pieces of the jigsaw and tell a coherent story. I summarise the scenario developed in this review below and in the sketch in Figure 4.

Jet feedback in star-forming galaxies produces interesting effects on all scales. This is because the jet plasma is efficiently shocked and isotropised by its interaction with molecular and other clouds. Dense gas on scales of tens of parsecs around a supermassive black hole may be compressed and accelerated, such that high-velocity stars are formed (Section 3). Complex interaction in the central kiloparsec leads to triggered star formation and outflows from this central zone (Section 3). Inclined radio sources can, of course, have more impact. The combination of central pressure and radio lobes surrounding the galaxy should then enhance star formation in the rest of the galaxy. Enhanced stellar feedback and the removal of dense halo gas may enhance gaseous outflows from those outer parts of the galaxy, such that eventually, most of the ISM takes part in the outflow. Emission line lobes

around smaller radio galaxies could be the observational manifestation of this. (Section 5). Even more emission line gases would be produced if galactic wind shells produced by a snow plough effect in a gaseous halo with the right conditions is overrun and turbulently entrained by the radio lobes (Section 6). The latter seems to happen frequently for massive high-redshift radio galaxies, but the general process is also found at a lower redshift for weaker radio sources. Eventually, radio lobes detach from the host galaxy, taking their load of metal-enriched gas with them to further spread it into the intergalactic medium. Approximately hydrostatic gas halos are probably present around galaxies above some mass. The hot halo has been clearly detected in the Milky Way. Jets likely contribute to heating these halos, and thus reduce the amount of fuel for star formation in the host galaxy.
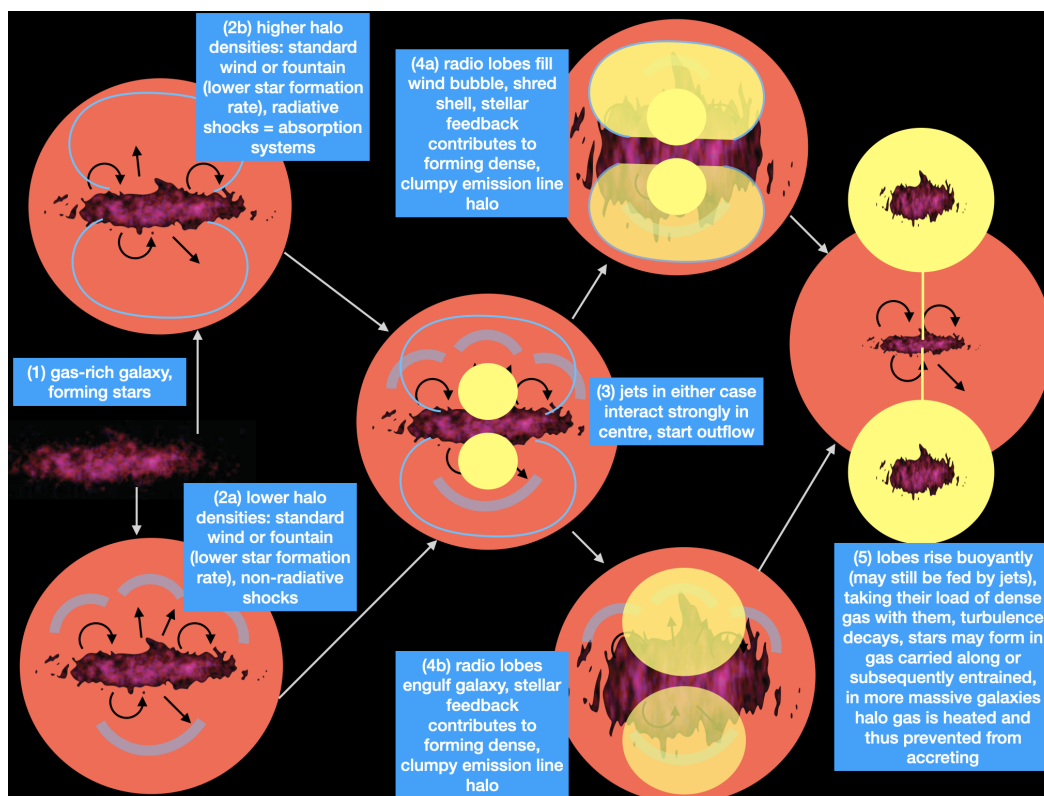

Figure 4. Sketch of the scenario of how jet feedback might work developed in this article. See Section 8 for more details.

Conflicts of Interest: The author declares no conflict of interest.

References

1. Magorrian, J.; Tremaine, S.; Richstone, D.; Bender, R.; Bower, G.; Dressler, A.; Faber, S.M.; Gebhardt, K.; Green, R.; Grillmair, C.; et al. The Demography of Massive Dark Objects in Galaxy Centers. *Astron. J.* **1998**, *115*, 2285–2305. [CrossRef]
2. Ferrarese, L.; Merritt, D. A Fundamental Relation between Supermassive Black Holes and Their Host Galaxies. *Astrophys. J.* **2000**, *539*, L9–L12. [CrossRef]
3. Häring, N.; Rix, H.W. On the Black Hole Mass-Bulge Mass Relation. *Astrophys. J.* **2004**, *604*, L89–L92. [CrossRef]
4. Onken, C.A.; Ferrarese, L.; Merritt, D.; Peterson, B.M.; Pogge, R.W.; Vestergaard, M.; Wandel, A. Supermassive Black Holes in Active Galactic Nuclei. II. Calibration of the Black Hole Mass-Velocity Dispersion Relationship for Active Galactic Nuclei. *Astrophys. J.* **2004**, *615*, 645–651. [CrossRef]
5. Gültekin, K.; Richstone, D.O.; Gebhardt, K.; Lauer, T.R.; Tremaine, S.; Aller, M.C.; Bender, R.; Dressler, A.; Faber, S.M.; Filippenko, A.V.; et al. The M-σ and M-L Relations in Galactic Bulges, and Determinations of Their Intrinsic Scatter. *Astrophys. J.* **2009**, *698*, 198–221. [CrossRef]

6. Bennert, V.N.; Auger, M.W.; Treu, T.; Woo, J.H.; Malkan, M.A. The Relation between Black Hole Mass and Host Spheroid Stellar Mass Out to z2. *Astrophys. J.* **2011**, *742*, 107. [CrossRef]

7. Bennert, V.N.; Treu, T.; Ding, X.; Stomberg, I.; Birrer, S.; Snyder, T.; Malkan, M.A.; Stephens, A.W.; Auger, M.W. A Local Baseline of the Black Hole Mass Scaling Relations for Active Galaxies. IV. Correlations Between M_{BH} and Host Galaxy σ, Stellar Mass, and Luminosity. *Astrophys. J.* **2021**, *921*, 36. [CrossRef]

8. Batiste, M.; Bentz, M.C.; Raimundo, S.I.; Vestergaard, M.; Onken, C.A. Recalibration of the M_{BH}-$\sigma_\star$ Relation for AGN. *Astrophys. J.* **2017**, *838*, L10. [CrossRef]

9. Bentz, M.C.; Manne-Nicholas, E. Black Hole – Galaxy Scaling Relationships for Active Galactic Nuclei with Reverberation Masses. *Astrophys. J.* **2018**, *864*, 1469. [CrossRef]

10. Silk, J.; Rees, M.J. Quasars and galaxy formation. *Astron. Astrophys.* **1998**, *331*, L1–L4.

11. King, A. The Supermassive Black Hole—Galaxy Connection. *Space Sci. Rev.* **2014**, *183*, 427–451. [CrossRef]

12. Çatmabacak, O.; Feldmann, R.; Anglés-Alcázar, D.; Faucher-Giguère, C.A.; Hopkins, P.F.; Kereš, D. Black hole-galaxy scaling relations in FIRE: The importance of black hole location and mergers. *Mon. Not. R. Astron. Soc.* **2022**, *511*, 506–535. [CrossRef]

13. Sijacki, D.; Vogelsberger, M.; Genel, S.; Springel, V.; Torrey, P.; Snyder, G.F.; Nelson, D.; Hernquist, L. The Illustris simulation: The evolving population of black holes across cosmic time. *Mon. Not. R. Astron. Soc.* **2015**, *452*, 575–596. [CrossRef]

14. Li, Y.; Habouzit, M.; Genel, S.; Somerville, R.; Terrazas, B.A.; Bell, E.F.; Pillepich, A.; Nelson, D.; Weinberger, R.; Rodriguez-Gomez, V.; et al. Correlations between Black Holes and Host Galaxies in the Illustris and IllustrisTNG Simulations. *Astrophys. J.* **2020**, *895*, 102. [CrossRef]

15. Ding, X.; Silverman, J.D.; Treu, T.; Li, J.; Bhowmick, A.K.; Menci, N.; Volonteri, M.; Blecha, L.; Matteo, T.D.; Dubois, Y. Concordance between Observations and Simulations in the Evolution of the Mass Relation between Supermassive Black Holes and Their Host Galaxies. *Astrophys. J.* **2022**, *933*, 132. [CrossRef]

16. Croton, D.J.; Springel, V.; White, S.D.M.; De Lucia, G.; Frenk, C.S.; Gao, L.; Jenkins, A.; Kauffmann, G.; Navarro, J.F.; Yoshida, N. The many lives of active galactic nuclei: Cooling flows, black holes and the luminosities and colours of galaxies. *Mon. Not. R. Astron. Soc.* **2006**, *365*, 11–28. [CrossRef]

17. Sijacki, D.; Springel, V.; Di Matteo, T.; Hernquist, L. A unified model for AGN feedback in cosmological simulations of structure formation. *Mon. Not. R. Astron. Soc.* **2007**, *380*, 877–900. [CrossRef]

18. Correa, C.A.; Schaye, J.; Trayford, J.W. The origin of the red-sequence galaxy population in the EAGLE simulation. *Mon. Not. R. Astron. Soc.* **2019**, *484*, 4401–4412. [CrossRef]

19. Davé, R.; Anglés-Alcázar, D.; Narayanan, D.; Li, Q.; Rafieferantsoa, M.H.; Appleby, S. SIMBA: Cosmological simulations with black hole growth and feedback. *Mon. Not. R. Astron. Soc.* **2019**, *486*, 2827–2849. [CrossRef]

20. Rodríguez Montero, F.; Davé, R.; Wild, V.; Anglés-Alcázar, D.; Narayanan, D. Mergers, starbursts, and quenching in the SIMBA simulation. *Mon. Not. R. Astron. Soc.* **2019**, *490*, 2139–2154. [CrossRef]

21. Davies, J.J.; Pontzen, A.; Crain, R.A. Galaxy mergers can initiate quenching by unlocking an AGN-driven transformation of the baryon cycle. *Mon. Not. R. Astron. Soc.* **2022**, *515*, 1430–1443. [CrossRef]

22. Xu, Y.; Luo, Y.; Kang, X.; Li, Z.; Li, Z.; Wang, P.; Libeskind, N. Quenching of Massive Disk Galaxies in the IllustrisTNG Simulation. *Astrophys. J.* **2022**, *928*, 100. [CrossRef]

23. Best, P.N.; Kaiser, C.R.; Heckman, T.M.; Kauffmann, G. AGN-controlled cooling in elliptical galaxies. *Mon. Not. R. Astron. Soc.* **2006**, *368*, L67–L71. [CrossRef]

24. Kaviraj, S.; Shabala, S.S.; Deller, A.T.; Middelberg, E. Radio AGN in spiral galaxies. *Mon. Not. R. Astron. Soc.* **2015**, *454*, 1595–1604. [CrossRef]

25. Turner, R.J.; Shabala, S.S. Energetics and Lifetimes of Local Radio Active Galactic Nuclei. *Astrophys. J.* **2015**, *806*, 59. [CrossRef]

26. Hardcastle, M.J.; Williams, W.L.; Best, P.N.; Croston, J.H.; Duncan, K.J.; Röttgering, H.J.A.; Sabater, J.; Shimwell, T.W.; Tasse, C.; Callingham, J.R.; et al. Radio-loud AGN in the first LoTSS data release. The lifetimes and environmental impact of jet-driven sources. *Astron. Astrophys.* **2019**, *622*, A12. [CrossRef]

27. Sabater, J.; Best, P.N.; Hardcastle, M.J.; Shimwell, T.W.; Tasse, C.; Williams, W.L.; Brüggen, M.; Cochrane, R.K.; Croston, J.H.; de Gasperin, F.; et al. The LoTSS view of radio AGN in the local Universe. The most massive galaxies are always switched on. *Astron. Astrophys.* **2019**, *622*, A17. [CrossRef]

28. Davis, F.; Kaviraj, S.; Hardcastle, M.J.; Martin, G.; Jackson, R.A.; Kraljic, K.; Malek, K.; Peirani, S.; Smith, D.J.B.; Volonteri, M.; et al. Radio AGN in nearby dwarf galaxies: The important role of AGN in dwarf galaxy evolution. *Mon. Not. R. Astron. Soc.* **2022**, *511*, 4109–4122. [CrossRef]

29. McNamara, B.R.; Nulsen, P.E.J. Heating Hot Atmospheres with Active Galactic Nuclei. *Annu. Rev. Astron. Astrophys.* **2007**, *45*, 117–175. [CrossRef]

30. Fabian, A.C. Observational Evidence of Active Galactic Nuclei Feedback. *Annu. Rev. Astron. Astrophys.* **2012**, *50*, 455–489. [CrossRef]

31. Hardcastle, M.J.; Croston, J.H. Radio galaxies and feedback from AGN jets. *New Astron. Rev.* **2020**, *88*, 101539. [CrossRef]

32. Reynolds, C.S.; Heinz, S.; Begelman, M.C. Shocks and Sonic Booms in the Intracluster Medium: X-ray Shells and Radio Galaxy Activity. *Astrophys. J.* **2001**, *549*, L179–L182. [CrossRef]

33. Krause, M. Very light jets II: Bipolar large scale simulations in King atmospheres. *Astron. Astrophys.* **2005**, *431*, 45–64. [CrossRef]

34. Dopita, M.A.; Groves, B.A.; Sutherland, R.S.; Binette, L.; Cecil, G. Are the Narrow-Line Regions in Active Galaxies Dusty and Radiation Pressure Dominated? *Astrophys. J.* **2002**, *572*, 753–761. [CrossRef]

35. Stern, J.; Laor, A.; Baskin, A. Radiation pressure confinement-I. Ionized gas in the ISM of AGN hosts. *Mon. Not. R. Astron. Soc.* **2014**, *438*, 901–921. [CrossRef]

36. Davies, R.L.; Dopita, M.A.; Kewley, L.; Groves, B.; Sutherland, R.; Hampton, E.J.; Shastri, P.; Kharb, P.; Bhatt, H.; Scharwächter, J.; et al. The Role of Radiation Pressure in the Narrow Line Regions of Seyfert Host Galaxies. *Astrophys. J.* **2016**, *824*, 50. [CrossRef]

37. Bianchi, S.; Guainazzi, M.; Laor, A.; Stern, J.; Behar, E. Evidence for radiation pressure compression in the X-ray narrow-line region of Seyfert galaxies. *Mon. Not. R. Astron. Soc.* **2019**, *485*, 416–427. [CrossRef]

38. Somalwar, J.; Johnson, S.D.; Stern, J.; Goulding, A.D.; Greene, J.E.; Zakamska, N.L.; Alexandroff, R.M.; Chen, H.W. Spatially Resolved UV Diagnostics of AGN Feedback: Radiation Pressure Dominates in a Prototypical Quasar-driven Superwind. *Astrophys. J.* **2020**, *890*, L28. [CrossRef]

39. Deconto-Machado, A.; Riffel, R.A.; Ilha, G.S.; Rembold, S.B.; Storchi-Bergmann, T.; Riffel, R.; Schimoia, J.S.; Schneider, D.P.; Bizyaev, D.; Feng, S.; et al. Ionised gas kinematics in MaNGA AGN. Extents of the narrow-line and kinematically disturbed regions. *Astron. Astrophys.* **2022**, *659*, A131. [CrossRef]

40. Schartmann, M.; Krause, M.; Burkert, A. Radiation feedback on dusty clouds during Seyfert activity. *Mon. Not. R. Astron. Soc.* **2011**, *415*, 741–752. [CrossRef]

41. Krause, M.; Schartmann, M.; Burkert, A. Magnetohydrodynamic stability of broad line region clouds. *Mon. Not. R. Astron. Soc.* **2012**, *425*, 3172–3187. [CrossRef]

42. Krumholz, M.R.; Thompson, T.A. Direct Numerical Simulation of Radiation Pressure-driven Turbulence and Winds in Star Clusters and Galactic Disks. *Astrophys. J.* **2012**, *760*, 155. [CrossRef]

43. Proga, D.; Waters, T. Cloud Formation and Acceleration in a Radiative Environment. *Astrophys. J.* **2015**, *804*, 137. [CrossRef]

44. Waters, T.; Proga, D. On the efficient acceleration of clouds in active galactic nuclei. *Mon. Not. R. Astron. Soc.* **2016**, *460*, L79–L83. [CrossRef]

45. Proga, D.; Waters, T.; Dyda, S.; Zhu, Z. Thermal Instability in Radiation Hydrodynamics: Instability Mechanisms, Position-dependent S-curves, and Attenuation Curves. *Astrophys. J.* **2022**, *935*, L37. [CrossRef]

46. Das, V.; Crenshaw, D.M.; Kraemer, S.B. Dynamics of the Narrow-Line Region in the Seyfert 2 Galaxy NGC 1068. *Astrophys. J.* **2007**, *656*, 699–708. [CrossRef]

47. Meena, B.; Crenshaw, D.M.; Schmitt, H.R.; Revalski, M.; Fischer, T.C.; Polack, G.E.; Kraemer, S.B.; Dashtamirova, D. Radiative Driving of the AGN Outflows in the Narrow-line Seyfert 1 Galaxy NGC 4051. *Astrophys. J.* **2021**, *916*, 31. [CrossRef]

48. Rawlings, S.; Jarvis, M.J. Evidence that powerful radio jets have a profound influence on the evolution of galaxies. *Mon. Not. R. Astron. Soc.* **2004**, *355*, L9–L12. [CrossRef]

49. Harris, D.E.; Carilli, C.L.; Perley, R.A. X-ray emission from the radio hotspots of Cygnus A. *Nature* **1994**, *367*, 713–716. [CrossRef]

50. Hardcastle, M.J.; Harris, D.E.; Worrall, D.M.; Birkinshaw, M. The Origins of X-Ray Emission from the Hot Spots of FR II Radio Sources. *Astrophys. J.* **2004**, *612*, 729–748. [CrossRef]

51. Sunada, Y.; Morimoto, A.; Tashiro, M.S.; Terada, Y.; Katsuda, S.; Sato, K.; Tateishi, D.; Sasaki, N. NuSTAR discovery of the hard X-ray emission and a wide-band X-ray spectrum from the Pictor A western hotspot. *Publ. Astron. Soc. Jpn.* **2022**, *74*, 602–611. [CrossRef]

52. Britzen, S.; Vermeulen, R.C.; Campbell, R.M.; Taylor, G.B.; Pearson, T.J.; Readhead, A.C.S.; Xu, W.; Browne, I.W.; Henstock, D.R.; Wilkinson, P. A multi-epoch VLBI survey of the kinematics of CFJ sources. II. Analysis of the kinematics. *Astron. Astrophys.* **2008**, *484*, 119–142. .:20077717. [CrossRef]

53. Lister, M.L.; Aller, M.F.; Aller, H.D.; Homan, D.C.; Kellermann, K.I.; Kovalev, Y.Y.; Pushkarev, A.B.; Richards, J.L.; Ros, E.; Savolainen, T. MOJAVE. X. Parsec-scale Jet Orientation Variations and Superluminal Motion in Active Galactic Nuclei. *Astron. J.* **2013**, *146*, 120. [CrossRef]

54. Lister, M.L.; Aller, M.F.; Aller, H.D.; Homan, D.C.; Kellermann, K.I.; Kovalev, Y.Y.; Pushkarev, A.B.; Richards, J.L.; Ros, E.; Savolainen, T. MOJAVE: XIII. Parsec-scale AGN Jet Kinematics Analysis Based on 19 years of VLBA Observations at 15 GHz. *Astron. J.* **2016**, *152*, 12. [CrossRef]

55. Lister, M.L.; Homan, D.C.; Hovatta, T.; Kellermann, K.I.; Kiehlmann, S.; Kovalev, Y.Y.; Max-Moerbeck, W.; Pushkarev, A.B.; Readhead, A.C.S.; Ros, E.; et al. MOJAVE. XVII. Jet Kinematics and Parent Population Properties of Relativistically Beamed Radio-loud Blazars. *Astrophys. J.* **2019**, *874*, 43. [CrossRef]

56. Lister, M. AGN Jet Kinematics on Parsec-Scales: The MOJAVE Program. *Galaxies* **2016**, *4*, 29. . 0029. [CrossRef]

57. Weaver, Z.R.; Jorstad, S.G.; Marscher, A.P.; Morozova, D.A.; Troitsky, I.S.; Agudo, I.; Gómez, J.L.; Lähteenmäki, A.; Tammi, J.; Tornikoski, M. Kinematics of Parsec-scale Jets of Gamma-Ray Blazars at 43 GHz during 10 yr of the VLBA-BU-BLAZAR Program. *Astrophys. J. Suppl. Ser.* **2022**, *260*, 12. [CrossRef]

58. Komissarov, S.S.; Barkov, M.V.; Vlahakis, N.; Königl, A. Magnetic acceleration of relativistic active galactic nucleus jets. *Mon. Not. R. Astron. Soc.* **2007**, *380*, 51–70. [CrossRef]

59. Porth, O.; Fendt, C. Acceleration and Collimation of Relativistic Magnetohydrodynamic Disk Winds. *Astrophys. J.* **2010**, *709*, 1100–1118. [CrossRef]

60. Gracia, J.; Vlahakis, N.; Agudo, I.; Tsinganos, K.; Bogovalov, S.V. Synthetic Synchrotron Emission Maps from MHD Models for the Jet of M87. *Astrophys. J.* **2009**, *695*, 503–510. [CrossRef]

61. Chatterjee, K.; Liska, M.; Tchekhovskoy, A.; Markoff, S.B. Accelerating AGN jets to parsec scales using general relativistic MHD simulations. *Mon. Not. R. Astron. Soc.* **2019**, *490*, 2200–2218. [CrossRef]

62. Alexander, P. Models of young powerful radio sources. *Mon. Not. R. Astron. Soc.* **2006**, *368*, 1404–1410. . 1365-2966.2006.10225.x. [CrossRef]

63. Krause, M.; Alexander, P.; Riley, J.; Hopton, D. A new connection between the jet opening angle and the large-scale morphology of extragalactic radio sources. *Mon. Not. R. Astron. Soc.* **2012**, *427*, 3196–32089. [CrossRef]

64. Bicknell, G.V. A model for the surface brightness of a turbulent low Mach number jet. I-Theoretical development and application to 3C 31. *Astrophys. J.* **1984**, *286*, 68–87. [CrossRef]

65. Massaglia, S.; Bodo, G.; Rossi, P.; Capetti, S.; Mignone, A. Making Faranoff-Riley I radio sources. I. Numerical hydrodynamic 3D simulations of low-power jets. *Astron. Astrophys.* **2016**, *596*, A12. [CrossRef]

66. Meisenheimer, K.; Yates, M.G.; Roeser, H.J. The synchrotron spectra of radio hot spots. II. Infrared imaging. *Astron. Astrophys.* **1997**, *325*, 57–73.

67. Hardcastle, M.J.; Croston, J.H.; Kraft, R.P. A Chandra Study of Particle Acceleration in the Multiple Hot Spots of Nearby Radio Galaxies. *Astrophys. J.* **2007**, *669*, 893–904. [CrossRef]

68. Norman, M.L.; Winkler, K.H.A.; Smarr, L.; Smith, M.D. Structure and dynamics of supersonic jets. *Astron. Astrophys.* **1982**, *113*, 285–302.

69. Alexander, P.; Pooley, G.G. *Cygnus A–Study of a Radio Galaxy*; Carilli, C.L., Harris, D.E., Eds.; Cambridge University Press: Cambridge, UK, 1996; p. 149.

70. Krause, M. Very light jets. I. Axisymmetric parameter study and analytic approximation. *Astron. Astrophys.* **2003**, *398*, 113–125. [CrossRef]

71. Gaibler, V.; Krause, M.; Camenzind, M. Very light magnetized jets on large scales-I. Evolution and magnetic fields. *Mon. Not. R. Astron. Soc.* **2009**, *400*, 1785–1802. [CrossRef]

72. Hardcastle, M.J.; Krause, M.G.H. Numerical modelling of the lobes of radio galaxies in cluster environments. *Mon. Not. R. Astron. Soc.* **2013**, *430*, 174–196. [CrossRef]

73. Hardcastle, M.J.; Krause, M.G.H. Numerical modelling of the lobes of radio galaxies in cluster environments-II. Magnetic field configuration and observability. *Mon. Not. R. Astron. Soc.* **2014**, *443*, 1482–1499. [CrossRef]

74. Iles, E.J.; Pettitt, A.R.; Okamoto, T. Differences in star formation activity between tidally triggered and isolated bars: A case study of NGC 4303 and NGC 3627. *Mon. Not. R. Astron. Soc.* **2022**, *510*, 3899–3916. [CrossRef]

75. Kennicutt, R.C.; Evans, N.J. Star Formation in the Milky Way and Nearby Galaxies. *Annu. Rev. Astron. Astrophys.* **2012**, *50*, 531–608. [CrossRef]

76. Armillotta, L.; Krumholz, M.R.; Di Teodoro, E.M.; McClure-Griffiths, N.M. The life cycle of the Central Molecular Zone-I. Inflow, star formation, and winds. *Mon. Not. R. Astron. Soc.* **2019**, *490*, 4401–4418. [CrossRef]

77. Narayan, C.A.; Jog, C.J. Vertical scaleheights in a gravitationally coupled, three-component Galactic disk. *Astron. Astrophys.* **2002**, *394*, 89–96. [CrossRef]

78. Langer, W.D.; Pineda, J.L.; Velusamy, T. The scale height of gas traced by [C ii] in the Galactic plane. *Astron. Astrophys.* **2014**, *564*, A101. [CrossRef]

79. Patra, N.N. H I scale height in spiral galaxies. *Mon. Not. R. Astron. Soc.* **2020**, *499*, 2063–2075. . 2959. [CrossRef]

80. Zheng, Y.; Wang, J.; Irwin, J.; Daniel Wang, Q.; Li, J.; English, J.; Ma, Q.; Wang, R.; Wang, K.; Krause, M.; et al. H I Vertical Structure of Nearby Edge-on Galaxies from CHANG-ES. *Res. Astron. Astrophys.* **2022**, *22*, 085004. [CrossRef]

81. Whittle, M.; Wilson, A.S. Jet-Gas Interactions in Markarian 78. I. Morphology and Kinematics. *Astron. J.* **2004**, *127*, 606–624. [CrossRef]

82. Mundell, C.G.; Wrobel, J.M.; Pedlar, A.; Gallimore, J.F. The Nuclear Regions of the Seyfert Galaxy NGC 4151: Parsec-Scale H I Absorption and a Remarkable Radio Jet. *Astrophys. J.* **2003**, *583*, 192–204. [CrossRef]

83. Das, V.; Crenshaw, D.M.; Kraemer, S.B.; Deo, R.P. Kinematics of the Narrow-Line Region in the Seyfert 2 Galaxy NGC 1068: Dynamical Effects of the Radio Jet. *Astron. J.* **2006**, *132*, 620–632. [CrossRef]

84. Rosario, D.J.; Whittle, M.; Nelson, C.H.; Wilson, A.S. The Radio Jet Interaction in NGC 5929: Direct Detection of Shocked Gas. *Astrophys. J.* **2010**, *711*, L94–L98. [CrossRef]

85. Riffel, R.A.; Storchi-Bergmann, T.; Riffel, R. Feeding versus feedback in active galactic nuclei from near-infrared integral field spectroscopy-X. NGC 5929. *Mon. Not. R. Astron. Soc.* **2015**, *451*, 3587–3605. [CrossRef]

86. Bicknell, G.V.; Mukherjee, D.; Wagner, A.Y.; Sutherland, R.S.; Nesvadba, N.P.H. Relativistic jet feedback-II. Relationship to gigahertz peak spectrum and compact steep spectrum radio galaxies. *Mon. Not. R. Astron. Soc.* **2018**, *475*, 3493–3501. [CrossRef]

87. O'Dea, C.P.; Saikia, D.J. Compact steep-spectrum and peaked-spectrum radio sources. *Astron. Astrophys. Rev.* **2021**, *29*, 3. [CrossRef]

88. Sutherland, R.S.; Bicknell, G.V. Interactions of a Light Hypersonic Jet with a Nonuniform Interstellar Medium. *Astrophys. J. Suppl. Ser.* **2007**, *173*, 37–69. [CrossRef]

89. Wagner, A.Y.; Bicknell, G.V. Relativistic Jet Feedback in Evolving Galaxies. *Astrophys. J.* **2011**, *728*, 29. [CrossRef]

90. Wagner, A.Y.; Bicknell, G.V.; Umemura, M. Driving Outflows with Relativistic Jets and the Dependence of Active Galactic Nucleus Feedback Efficiency on Interstellar Medium Inhomogeneity. *Astrophys. J.* **2012**, *757*, 136. [CrossRef]

91. Mukherjee, D.; Bicknell, G.V.; Sutherland, R.; Wagner, A. Relativistic jet feedback in high-redshift galaxies-I. Dynamics. *Mon. Not. R. Astron. Soc.* **2016**, *461*, 967–983. [CrossRef]

92. Mukherjee, D.; Bicknell, G.V.; Wagner, A.Y.; Sutherland, R.S.; Silk, J. Relativistic jet feedback-III. Feedback on gas discs. *Mon. Not. R. Astron. Soc.* **2018**, *479*, 5544–5566. [CrossRef]

93. Mandal, A.; Mukherjee, D.; Federrath, C.; Nesvadba, N.P.H.; Bicknell, G.V.; Wagner, A.Y.; Meenakshi, M. Impact of relativistic jets on the star formation rate: A turbulence-regulated framework. *Mon. Not. R. Astron. Soc.* **2021**, *508*, 4738–4757. [CrossRef]

94. Meenakshi, M.; Mukherjee, D.; Wagner, A.Y.; Nesvadba, N.P.H.; Bicknell, G.V.; Morganti, R.; Janssen, R.M.J.; Sutherland, R.S.; Mandal, A. Modelling observable signatures of jet-ISM interaction: Thermal emission and gas kinematics. *Mon. Not. R. Astron. Soc.* **2022**, *516*, 766–786. [CrossRef]

95. Mukherjee, D.; Wagner, A.Y.; Bicknell, G.V.; Morganti, R.; Oosterloo, T.; Nesvadba, N.; Sutherland, R.S. The jet-ISM interactions in IC 5063. *Mon. Not. R. Astron. Soc.* **2018**, *476*, 80–95. [CrossRef]

96. Krause, M.G.H.; Gaibler, V. AGN Feedback in Galaxy Formation. In Proceedings of the AGN Feedback in Galaxy Formation, Workshop, Vulcano, Italy, 18–22 May 2008; Antonuccio-Delogu, V., Silk, J., Eds.; Cambridge University Press: Cambridge, UK, 2010; pp. 183–193; ISBN 9780521192545. [CrossRef]

97. Meenakshi, M.; Mukherjee, D.; Wagner, A.Y.; Nesvadba, N.P.H.; Morganti, R.; Janssen, R.M.J.; Bicknell, G.V. The extent of ionization in simulations of radio-loud AGNs impacting kpc gas discs. *Mon. Not. R. Astron. Soc.* **2022**, *511*, 1622–1636. [CrossRef]

98. Gaibler, V.; Khochfar, S.; Krause, M. Asymmetries in extragalactic double radio sources: Clues from 3D simulations of jet-disc interaction. *Mon. Not. R. Astron. Soc.* **2011**, *411*, 155–161. [CrossRef]

99. Jeffreson, S.M.R.; Sun, J.; Wilson, C.D. On the scale height of the molecular gas disc in Milky Way-like galaxies. *Mon. Not. R. Astron. Soc.* **2022**, *515*, 1663–1675. [CrossRef]

100. Silk, J.; Antonuccio-Delogu, V.; Dubois, Y.; Gaibler, V.; Haas, M.R.; Khochfar, S.; Krause, M. Jet interactions with a giant molecular cloud in the Galactic centre and ejection of hypervelocity stars. *Astron. Astrophys.* **2012**, *545*, L11. [CrossRef]

101. Chen, Y.M.; Shi, Y.; Wild, V.; Tremonti, C.; Rowlands, K.; Bizyaev, D.; Yan, R.; Lin, L.; Riffel, R. Post-starburst galaxies in SDSS-IV MaNGA. *Mon. Not. R. Astron. Soc.* **2019**, *489*, 5709–5722. [CrossRef]

102. Otter, J.A.; Rowlands, K.; Alatalo, K.; Leung, H.H.; Wild, V.; Luo, Y.; Petric, A.O.; Sazonova, E.; Stark, D.V.; Heckman, T.; et al. Resolved Molecular Gas Observations of MaNGA Post-starbursts Reveal a Tumultuous Past. *Astrophys. J.* **2022**, *941*, 93. [CrossRef]

103. Kaviraj, S.; Kirkby, L.A.; Silk, J.; Sarzi, M. The UV properties of E+A galaxies: Constraints on feedback-driven quenching of star formation. *Mon. Not. R. Astron. Soc.* **2007**, *382*, 960–970. [CrossRef]

104. Kaviraj, S.; Shabala, S.S.; Deller, A.T.; Middelberg, E. The triggering of local AGN and their role in regulating star formation. *Mon. Not. R. Astron. Soc.* **2015**, *452*, 774–783. [CrossRef]

105. Krause, M.G.H.; Hardcastle, M.J.; Shabala, S.S. Probing gaseous halos of galaxies with radio jets. *Astron. Astrophys.* **2019**, *627*, A113. [CrossRef]

106. Bovy, J.; Rix, H.W. A Direct Dynamical Measurement of the Milky Way's Disk Surface Density Profile, Disk Scale Length, and Dark Matter Profile at 4 kpc $\leq$ R $\leq$ 9 kpc. *Astrophys. J.* **2013**, *779*, 115. [CrossRef]

107. Taylor, C.; Boylan-Kolchin, M.; Torrey, P.; Vogelsberger, M.; Hernquist, L. The mass profile of the Milky Way to the virial radius from the Illustris simulation. *Mon. Not. R. Astron. Soc.* **2016**, *461*, 3483–3493. [CrossRef]

108. Gupta, A.; Mathur, S.; Krongold, Y.; Nicastro, F.; Galeazzi, M. A Huge Reservoir of Ionized Gas around the Milky Way: Accounting for the Missing Mass? *Astrophys. J.* **2012**, *756*, L8. [CrossRef]

109. Su, M.; Slatyer, T.R.; Finkbeiner, D.P. Giant Gamma-ray Bubbles from Fermi-LAT: Active Galactic Nucleus Activity or Bipolar Galactic Wind? *Astrophys. J.* **2010**, *724*, 1044–1082. [CrossRef]

110. Yang, H.Y.K.; Ruszkowski, M.; Ricker, P.M.; Zweibel, E.; Lee, D. The Fermi Bubbles: Supersonic Active Galactic Nucleus Jets with Anisotropic Cosmic-Ray Diffusion. *Astrophys. J.* **2012**, *761*, 185. [CrossRef]

111. Predehl, P.; Sunyaev, R.A.; Becker, W.; Brunner, H.; Burenin, R.; Bykov, A.; Cherepashchuk, A.; Chugai, N.; Churazov, E.; Doroshenko, V.; et al. Detection of large-scale X-ray bubbles in the Milky Way halo. *Nature* **2020**, *588*, 227–231. [CrossRef]

112. Yang, H.Y.K.; Ruszkowski, M.; Zweibel, E.G. Fermi and eROSITA bubbles as relics of the past activity of the Galaxy's central black hole. *Nat. Astron.* **2022**, *6*, 584–591. [CrossRef]

113. Mingo, B.; Hardcastle, M.J.; Croston, J.H.; Evans, D.A.; Kharb, P.; Kraft, R.P.; Lenc, E. Shocks, Seyferts, and the Supernova Remnant Connection: A Chandra Observation of the Circinus Galaxy. *Astrophys. J.* **2012**, *758*, 95. [CrossRef]

114. Pshirkov, M.S.; Vasiliev, V.V.; Postnov, K.A. Evidence of Fermi bubbles around M31. *Mon. Not. R. Astron. Soc.* **2016**, *459*, L76–L80. [CrossRef]

115. Hodges-Kluck, E.J.; Bregman, J.N.; Li, J.t. The Hot, Accreted Halo of NGC 891. *Astrophys. J.* **2018**, *866*, 126. [CrossRef]

116. Cecil, G.; Bland-Hawthorn, J.; Veilleux, S. Tightly Correlated X-Ray/Hα-emitting Filaments in the Superbubble and Large-Scale Superwind of NGC 3079. *Astrophys. J.* **2002**, *576*, 745–752. [CrossRef]

117. Owen, E.R.; Yang, H.Y.K. Emission from hadronic and leptonic processes in galactic jet-driven bubbles. *Mon. Not. R. Astron. Soc.* **2022**, *516*, 1539–1556. [CrossRef]

118. Smith, D.J.B.; Krause, M.G.; Hardcastle, M.J.; Drake, A.B. Relic jet activity in 'Hanny's Voorwerp' revealed by the LOFAR two metre sky survey. *Mon. Not. R. Astron. Soc.* **2022**, *514*, 3879–3885. [CrossRef]

119. Nesvadba, N.P.H.; Wagner, A.Y.; Mukherjee, D.; Mandal, A.; Janssen, R.M.J.; Zovaro, H.; Neumayer, N.; Bagchi, J.; Bicknell, G. Jet-driven AGN feedback on molecular gas and low star-formation efficiency in a massive local spiral galaxy with a bright X-ray halo. *Astron. Astrophys.* **2021**, *654*, A8. [CrossRef]

120. Van Ojik, R.; Röttgering, H.J.A.; Miley, G.K.; Hunstead, R.W. The gaseous environments of radio galaxies in the early Universe: kinematics of the Lyman *α* emission and spatially resolved H I absorption. *Astron. Astrophys.* **1997**, *317*, 358–384.

121. Gaibler, V.; Khochfar, S.; Krause, M.; Silk, J. Jet-induced star formation in gas-rich galaxies. *Mon. Not. R. Astron. Soc.* **2012**, *425*, 438–449. [CrossRef]

122. Bieri, R.; Dubois, Y.; Silk, J.; Mamon, G.A.; Gaibler, V. External pressure-triggering of star formation in a disc galaxy: A template for positive feedback. *Mon. Not. R. Astron. Soc.* **2016**, *455*, 4166–4182. [CrossRef]

123. De Young, D.S. Star formation in radio galaxies at large redshift. *Astrophys. J.* **1989**, *342*, L59–L62. [CrossRef]

124. Antonuccio-Delogu, V.; Silk, J. AGN Jet-induced Feedback in Galaxies. I. Suppression of Star Formation. *Mon. Not. R. Astron. Soc.* 2008, *in press*. [CrossRef]

125. Tortora, C.; Antonuccio-Delogu, V.; Kaviraj, S.; Silk, J.; Romeo, A.D.; Becciani, U. AGN jet-induced feedback in galaxies-II. Galaxy colours from a multicloud simulation. *Mon. Not. R. Astron. Soc.* **2009**, *396*, 61–77. [CrossRef]

126. Krause, M.; Alexander, P. Simulations of multiphase turbulence in jet cocoons. *Mon. Not. R. Astron. Soc.* **2007**, *376*, 465–478. [CrossRef]

127. Krause, M.G.H. Jets and multi-phase turbulence. *MmSAI* **2008**, *79*, 1162.

128. McCarthy, P.J. High redshift radio galaxies. *Annu. Rev. Astron. Astrophys.* **1993**, *31*, 639–688. [CrossRef]

129. Miley, G.; De Breuck, C. Distant radio galaxies and their environments. *Astron. Astrophys. Rev.* **2008**, *15*, 67–144. [CrossRef]

130. Nesvadba, N.P.H.; Lehnert, M.D.; De Breuck, C.; Gilbert, A.M.; van Breugel, W. Evidence for powerful AGN winds at high redshift: Dynamics of galactic outflows in radio galaxies during the "Quasar Era". *Astron. Astrophys.* **2008**, *491*, 407–424. .:200810346. [CrossRef]

131. Meisenheimer, K.; Hippelein, H. The emission-line lobes of 3C 368. *Astron. Astrophys.* **1992**, *264*, 455–471.

132. Best, P.N.; Longair, M.S.; Roettgering, J.H.A. HST, radio and infrared observations of 28 3CR radio galaxies at redshift Z of about 1. I-The observations. *Mon. Not. R. Astron. Soc.* **1997**, *292*, 758–794. [CrossRef]

133. Best, P.N.; Röttgering, H.J.A.; Longair, M.S. Ionization, shocks and evolution of the emission-line gas of distant 3CR radio galaxies. *Mon. Not. R. Astron. Soc.* **2000**, *311*, 23–36. [CrossRef]

134. Yates-Jones, P.M.; Turner, R.J.; Shabala, S.S.; Krause, M.G.H. PRAiSE: Resolved spectral evolution in simulated radio sources. *Mon. Not. R. Astron. Soc.* **2022**, *511*, 5225–5240. [CrossRef]

135. Chon, G.; Böhringer, H.; Krause, M.; Trümper, J. Discovery of an X-ray cavity near the radio lobes of Cygnus A indicating previous AGN activity. *Astron. Astrophys.* **2012**, *545*, L3. [CrossRef]

136. McKean, J.P.; Godfrey, L.E.H.; Vegetti, S.; Wise, M.W.; Morganti, R.; Hardcastle, M.J.; Rafferty, D.; Anderson, J.; Avruch, I.M.; Beck, R.; et al. LOFAR imaging of Cygnus A-direct detection of a turnover in the hotspot radio spectra. *Mon. Not. R. Astron. Soc.* **2016**, *463*, 3143–3150. [CrossRef]

137. Privon, G.C.; Baum, S.A.; O'Dea, C.P.; Gallimore, J.; Noel-Storr, J.; Axon, D.J.; Robinson, A. Modeling the Infrared Emission in Cygnus A. *Astrophys. J.* **2012**, *747*, 46. [CrossRef]

138. Heath, D.; Krause, M.; Alexander, P. Chemical enrichment of the intracluster medium by FR II radio sources. *Mon. Not. R. Astron. Soc.* **2007**, *374*, 787–792. [CrossRef]

139. Dubois, Y.; Teyssier, R. On the onset of galactic winds in quiescent star forming galaxies. *Astron. Astrophys.* **2008**, *477*, 79–94. [CrossRef]

140. von Glasow, W.; Krause, M.G.H.; Sommer-Larsen, J.; Burkert, A. Galactic winds-how to launch galactic outflows in typical Lyman-break galaxies. *Mon. Not. R. Astron. Soc.* **2013**, *434*, 1151–1170. [CrossRef]

141. Rodgers-Lee, D.; Krause, M.G.H.; Dale, J.; Diehl, R. Synthetic ^{26}Al emission from galactic-scale superbubble simulations. *Mon. Not. R. Astron. Soc.* **2019**, *490*, 1894–1912. [CrossRef]

142. Dey, A.; van Breugel, W.; Vacca, W.D.; Antonucci, R. Triggered Star Formation in a Massive Galaxy at Z = 3.8: 4C 41.17. *Astrophys. J.* **1997**, *490*, 698. [CrossRef]

143. Bicknell, G.V.; Sutherland, R.S.; van Breugel, W.J.M.; Dopita, M.A.; Dey, A.; Miley, G.K. Jet-induced Emission-Line Nebulosity and Star Formation in the High-Redshift Radio Galaxy 4C 41.17. *Astrophys. J.* **2000**, *540*, 678–686. [CrossRef]

144. Jarvis, M.E.; Harrison, C.M.; Mainieri, V.; Alexander, D.M.; Arrigoni Battaia, F.; Calistro Rivera, G.; Circosta, C.; Costa, T.; De Breuck, C.; Edge, A.C.; et al. The quasar feedback survey: Discovering hidden Radio-AGN and their connection to the host galaxy ionized gas. *Mon. Not. R. Astron. Soc.* **2021**, *503*, 1780–1797. [CrossRef]

145. Jimenez-Gallardo, A.; Sani, E.; Ricci, F.; Mazzucchelli, C.; Balmaverde, B.; Massaro, F.; Capetti, A.; Forman, W.R.; Kraft, R.P.; Venturi, G.; et al. The Cavity of 3C 196.1: H*α* Emission Spatially Associated with an X-Ray Cavity. *Astrophys. J.* **2022**, *941*, 114. [CrossRef]

146. De Breuck, C.; Röttgering, H.; Miley, G.; van Breugel, W.; Best, P. A statistical study of emission lines from high redshift radio galaxies. *Astron. Astrophys.* **2000**, *362*, 519–543.

147. Jarvis, M.J.; Wilman, R.J.; Röttgering, H.J.A.; Binette, L. Probing the absorbing haloes around two high-redshift radio galaxies with VLT-UVES*. *Mon. Not. R. Astron. Soc.* **2003**, *338*, 263–272. [CrossRef]

148. Swinbank, A.M.; Vernet, J.D.R.; Smail, I.; De Breuck, C.; Bacon, R.; Contini, T.; Richard, J.; Röttgering, H.J.A.; Urrutia, T.; Venemans, B. Mapping the dynamics of a giant Ly α halo at z = 4.1 with MUSE: The energetics of a large-scale AGN-driven outflow around a massive, high-redshift galaxy. *Mon. Not. R. Astron. Soc.* **2015**, *449*, 1298–1308. [CrossRef]

149. Kolwa, S.; Vernet, J.; De Breuck, C.; Villar-Martín, M.; Humphrey, A.; Arrigoni-Battaia, F.; Gullberg, B.; Falkendal, T.; Drouart, G.; Lehnert, M.D.; et al. MUSE unravels the ionisation and origin of metal-enriched absorbers in the gas halo of a z = 2.92 radio galaxy. *Astron. Astrophys.* **2019**, *625*, A102. [CrossRef]

150. Wang, W.; Wylezalek, D.; De Breuck, C.; Vernet, J.; Humphrey, A.; Villar Martín, M.; Lehnert, M.D.; Kolwa, S. Mapping the "invisible" circumgalactic medium around a z ∼ 4.5 radio galaxy with MUSE. *Astron. Astrophys.* **2021**, *654*, A88. [CrossRef]

151. Krause, M. Galactic wind shells and high redshift radio galaxies. On the nature of associated absorbers. *Astron. Astrophys.* **2005**, *436*, 845–851. [CrossRef]

152. Binette, L.; Kurk, J.D.; Villar-Martín, M.; Röttgering, H.J.A. A vestige low metallicity gas shell surrounding the radio galaxy 0943-242 at z = 2.92. *Astron. Astrophys.* **2000**, *356*, 23–32.

153. Binette, L.; Wilman, R.J.; Villar-Martín, M.; Fosbury, R.A.E.; Jarvis, M.J.; Röttgering, H.J.A. Ionization of large-scale absorbing haloes and feedback events from high-redshift radio galaxies. *Astron. Astrophys.* **2006**, *459*, 31–42.. [CrossRef]

154. Krause, M. Absorbers and Globular Cluster Formation in Powerful High Redshift Radio Galaxies. *Astron. Astrophys.* **2002**, *386*, L1–L4. [CrossRef]

155. Schaerer, D.; Verhamme, A. 3D Lyα radiation transfer. II. Fitting the Lyman break galaxy MS 1512-cB58 and implications for Lyα emission in high-z starbursts. *Astron. Astrophys.* **2008**, *480*, 369–377. [CrossRef]

156. Verhamme, A.; Schaerer, D.; Atek, H.; Tapken, C. 3D Lyα radiation transfer. III. Constraints on gas and stellar properties of z ˜ 3 Lyman break galaxies (LBG) and implications for high-z LBGs and Lyα emitters. *Astron. Astrophys.* **2008**, *491*, 89–111. [CrossRef]

157. Schaerer, D.; Hayes, M.; Verhamme, A.; Teyssier, R. Grid of Lyα radiation transfer models for interpreting distant galaxies. *Astron. Astrophys.* **2011**, *531*, A12. [CrossRef]

158. Hashimoto, T.; Verhamme, A.; Ouchi, M.; Shimasaku, K.; Schaerer, D.; Nakajima, K.; Shibuya, T.; Rauch, M.; Ono, Y.; Goto, R. A Close Comparison between Observed and Modeled Lyα Lines for z2.2 Lyα Emitters. *Astrophys. J.* **2015**, *812*, 157. [CrossRef]

159. Birnboim, Y.; Dekel, A. Virial shocks in galactic haloes? *Mon. Not. R. Astron. Soc.* **2003**, *345*, 349–364. [CrossRef]

160. Babul, A.; Sharma, P.; Reynolds, C.S. Isotropic Heating of Galaxy Cluster Cores via Rapidly Reorienting Active Galactic Nucleus Jets. *Astrophys. J.* **2013**, *768*, 11. [CrossRef]

161. Yang, H.Y.K.; Reynolds, C.S. How AGN Jets Heat the Intracluster Medium—Insights from Hydrodynamic Simulations. *Astrophys. J.* **2016**, *829*, 90. [CrossRef]

162. Krause, M.G.H.; Shabala, S.S.; Hardcastle, M.J.; Bicknell, G.V.; Böhringer, H.; Chon, G.; Nawaz, M.A.; Sarzi, M.; Wagner, A.Y. How frequent are close supermassive binary black holes in powerful jet sources? *Mon. Not. R. Astron. Soc.* **2019**, *482*, 240–261. [CrossRef]

163. Shabala, S.S.; Jurlin, N.; Morganti, R.; Brienza, M.; Hardcastle, M.J.; Godfrey, L.E.H.; Krause, M.G.H.; Turner, R.J. The duty cycle of radio galaxies revealed by LOFAR: Remnant and restarted radio source populations in the Lockman Hole. *Mon. Not. R. Astron. Soc.* **2020**, *496*, 1706–1717. [CrossRef]

164. Fabian, A.C.; Reynolds, C.S.; Taylor, G.B.; Dunn, R.J.H. On viscosity, conduction and sound waves in the intracluster medium. *Mon. Not. R. Astron. Soc.* **2005**, *363*, 891–896. [CrossRef]

165. Wang, S.C.; Yang, H.Y.K. Production efficiencies of sound waves in the intracluster medium driven by AGN jets. *Mon. Not. R. Astron. Soc.* **2022**, *512*, 5100–5109. [CrossRef]

166. Iqbal, A.; Majumdar, S.; Nath, B.B.; Roychowdhury, S. Heating of the intracluster medium by buoyant bubbles and sound waves. *Mon. Not. R. Astron. Soc.* **2023**, *518*, 2735–2745. [CrossRef]

167. Raouf, M.; Shabala, S.S.; Croton, D.J.; Khosroshahi, H.G.; Bernyk, M. The many lives of active galactic nuclei-II: The formation and evolution of radio jets and their impact on galaxy evolution. *Mon. Not. R. Astron. Soc.* **2017**, *471*, 658–670. [CrossRef]

168. van Ojik, R.; Röttgering, H.J.A.; Carilli, C.L.; Miley, G.K.; Bremer, M.N.; Macchetto, F. A powerful radio galaxy at z = 3.6 in a giant rotating Lyman α halo. *Astron. Astrophys.* **1996**, *313*, 25–44.

169. Reuland, M.; van Breugel, W.; de Vries, W.; Dopita, M.A.; Dey, A.; Miley, G.; Röttgering, H.; Venemans, B.; Stanford, S.A.; Lacy, M.; et al. Metal-Enriched Gaseous Halos around Distant Radio Galaxies: Clues to Feedback in Galaxy Formation. *Astron. J.* **2007**, *133*, 2607–2623. [CrossRef]

170. Pentericci, L.; McCarthy, P.J.; Röttgering, H.J.A.; Miley, G.K.; van Breugel, W.J.M.; Fosbury, R. NICMOS Observations of High-Redshift Radio Galaxies: Witnessing the Formation of Bright Elliptical Galaxies? *Astrophys. J. Suppl. Ser.* **2001**, *135*, 63–85. [CrossRef]

171. Reuland, M.; van Breugel, W.; Röttgering, H.; de Vries, W.; Stanford, S.A.; Dey, A.; Lacy, M.; Bland-Hawthorn, J.; Dopita, M.; Miley, G. Giant Lyα Nebulae Associated with High-Redshift Radio Galaxies. *Astrophys. J.* **2003**, *592*, 755–766. [CrossRef]